Tilted Fiber Bragg Grating in Graded-Index Multimode Fiber and Its Sensing Characteristics

Dengyong LI, Yuan GONG[*], and Yu WU

Key Lab of Optical Fiber Sensing & Communications (Ministry of Education), University of Electronic Science and Technology of China, Chengdu, 611731, China

*Corresponding author: Yuan GONG   E-mail: ofsgon@gmail.com

Abstract: Tilted fiber Bragg grating (TFBG) and reflective tilted fiber Bragg grating (R-TFBG) were proposed and demonstrated in the graded-index multimode fiber (GI-MMF). The TFBGs with grating planes tilted at an angle of 2.5° corresponding to the fiber axis were inscribed. The TFBGs in the GI-MMF had the good linear sensitivity to the temperature, strain and curvature. The fiber was then cleaved at the far end of the TFBG to form an R-TFBG using the Fresnel reflection of the fiber end. The reflective spectra of the R-TFBG were given, and the temperature sensing properties were also investigated.

Keywords: TFBG, GI-MMF, sensor

1. Introduction

Tilted fiber Bragg grating (TFBG) have been extensively investigated in recent years due to its unique properties in the field of sensing [1–12]. Bragg gratings in multimode fibers (MMFs) have also attracted much attention. Wanseret *et al*. [13] calculated the spectrum of a Bragg grating in the MMF and also used it as a bend sensor. Mizunami *et al*. [14] experimentally reported the spectral properties of MMF gratings and investigated the temperature sensing performance and the polarization characteristics. Szkopek [15] proposed a novel multimode fiber structure with modal propagation characteristics tailored to facilitate the creation of narrowband high-reflectivity fiber Bragg gratings. Zhou *et al*. [16] experimentally showed that the radiation pattern of the multimode TFBG was more restricted than the single ones. Yang *et al*. [17] fabricated TFBGs with different tilt angles and observed some unique features of the multimode TFBG. Chen *et al*. [18] made the thinner clad of the multimode TFBG using hydrofluoric acid (HF) acid corrosion and found out that the higher order modes were much more sensitive than the low order modes to the external refractive index.

In most experiments, the transmission spectra of the TFBG were detected, and the wavelength shift of the notches in the transmission spectra was then employed for the sensing of various parameters [1–3]. Another commonly-used method is to re-couple the backward cladding mode into the

lead-in single mode fiber via core-offset coupling [4, 5], employing a short section of the multimode fiber [6, 7] or an optical fiber taper [8]. The structure is relatively complex and not flexible enough for the applications that require the small size of the sensor. In this paper, two kinds of TFBG sensors are fabricated based on the graded-index multimode fiber, and the sensing properties are fully explored.

2. Sensor fabrication and its sensing characteristics

In the first experiment, the TFBG was fabricated in a singlemode-multimode-singlemode (SMS) fiber structure, similar to that in [19], as shown schematically in Fig. 1. The TFBG had a length of 10 mm, and both ends had an additional 20-cm graded-index multimode fiber (GI-MMF). Both ends were respectively fusion spliced to single mode fibers (SMFs).
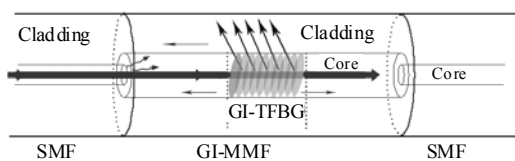
Fig. 1 Schematic diagram of the TFBG structure and principle of operation.

By using the 248-nm KrF excimer laser (BraggStar Industrial-1 000-248 nm-FT, Coherent, Inc.), TFBGs were fabricated in th hydrogen-loaded GI-MMF, which had a core diameter of 62.5 μm. The hydrogen loading was performed with a pressure of 120 bar and 70 ℃ for 3 days. The ultraviolet (UV) laser beam with a size of 3.5 mm× 7 mm, which was expanded by a beam telescope and then converged to the fiber right behind the phase mask. The uniform phase mask has a period of 1074.6 nm. We fabricated 2.5° slanted gratings with an exposure time of 45 seconds, with the laser operating at a rate of 100 Hz and 6mJ per pulse. The spectrum was monitored by an optical spectrum analyzer (Si720, Micron Optics Inc.) with a resolution of 1 pm. The transmission spectrum of the GI-TFBG was shown in Fig. 2.
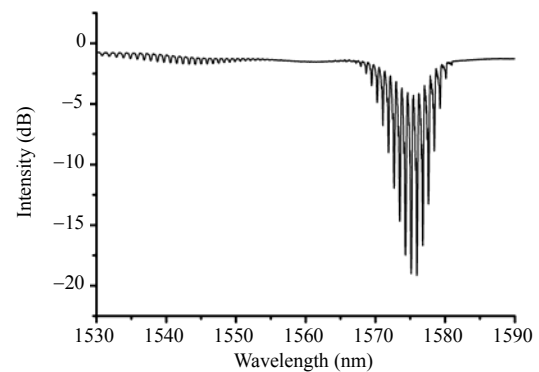
Fig. 2 Transmission spectra of 2.5° GI-TFBG.

The sensing performance of the GI-TFBG was evaluated by a series of experiments. First, we put the GI-TFBG into a temperature test chamber (WD7005) and recorded the transmission spectra every 20 ℃ raised from the room temperature (26 ℃) to 106 ℃. We found that the wavelength shift of each peak in the transmission spectrum was the same, so we selected the transmission peak with the maximum fringe contrast to do the temperature measurement. The wavelength shift as a function of the temperature is shown in Fig. 3. The temperature sensitivity of 11 pm/℃ and a linearity of 0.99882 were obtained. The strain and curvature responses were also measured. The strain sensitivity and curvature sensitivity were 0.77 pm/με and 21 pm/m^{-1}, as shown in Figs. 4 and 5, respectively. The strain linearity and curvature linearity were 0.9999 and 0.9997, respectively. High sensitivity measurement of the curvature over a large scale could be obtained.
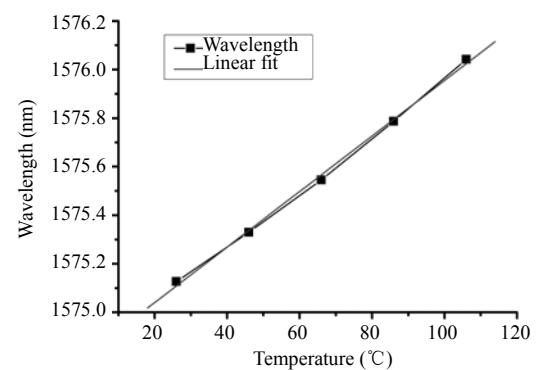
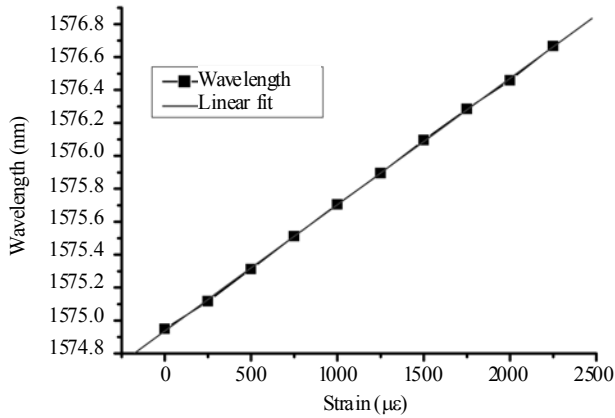Fig. 3 Wavelength shift as a function of the temperature.

Fig. 4 Wavelength shift of the transmission spectrum of the GI-TFBG under different strain.
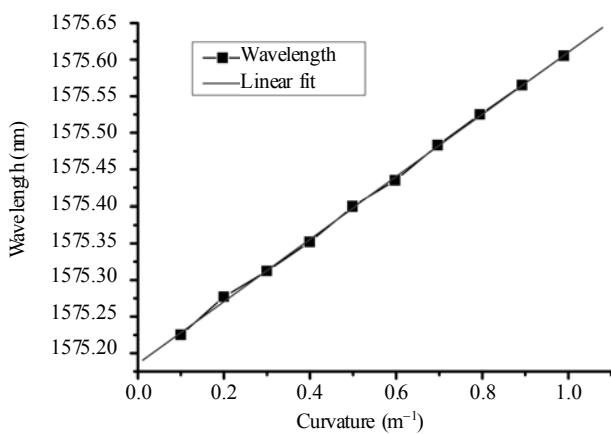

Fig. 5 Wavelength shift of the transmission spectrum of the GI-TFBG under different curvature.

In order to make sensors with a smaller size, the reflective TFBG (R-TFBG) sensor was developed by using the Fresnel reflection of the fiber end. The sensor had a simple fiber tip structure, and only the reflective spectrum was measured for the temperature measurement. The TFBG was inscribed in the GI-MMF using the same fabrication process and laser parameters. After the inscription of the TFBGs, the far end was cleaved to form the R-TFBGs by introducing the Fresnel reflection of the fiber end. Figure 6 shows the schematic diagram of the R-TFBGs on the standard SMF or GI-MMF. It took about 2 minutes of the UV-laser exposure to fabricate a TFBG in the SMF while about only 45 seconds to fabricate a TFBG with a similar

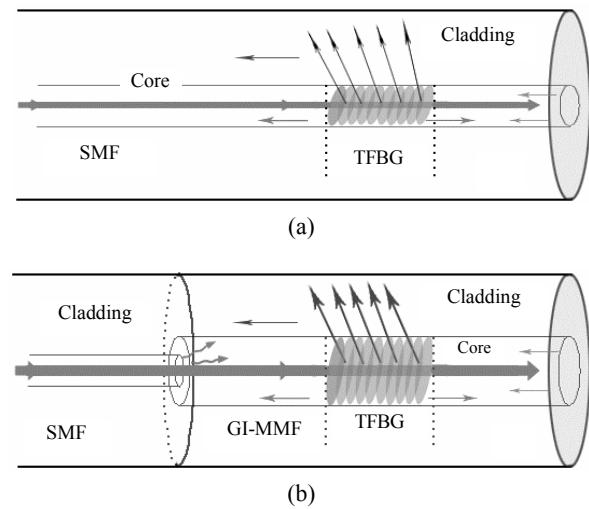reflectivity in the GI-MMF, due to the higher doping concentration of Ge in the latter.

Fig. 6 Schematic diagram of two R-TFBG sensor structures in the (a) SMF and (b) GI-MMF.

The reflective spectra of the two R-TFBGs were recorded by an optical spectrum analyzer (OSA), as shown in Fig. 7. In the short wavelength range of the reflective spectrum of the R-TFBG in th SMF, the wavelength notches were similar to that in the transmission spectrum of a typical TFBG, except for a certain number of losses during the reflection on the fiber end. The contrast of the resonant notches almost doubled as the reflected light transmitted through the TFBG twice. The Bragg reflection was still observed in Fig. 7(a) as the reflectivity of the TFBG at the Bragg wavelength was much higher than that of the Fresnel reflection. In the GI-MMF R-TFBG sensor, there was a sequence of resonant notches corresponding to different orders of the core mode in the GI-MMF, as shown in Fig. 7(b). Before cleaving the far end of the TFBGs in the SMF and GI-MMF, the Bragg wavelengths were determined to be 1557.1 nm and 1582.4 nm, respectively, from the reflective spectra. The effective indices of the core mode in two kinds of fibers were further calculated to be 1.449 and 1.472, respectively.
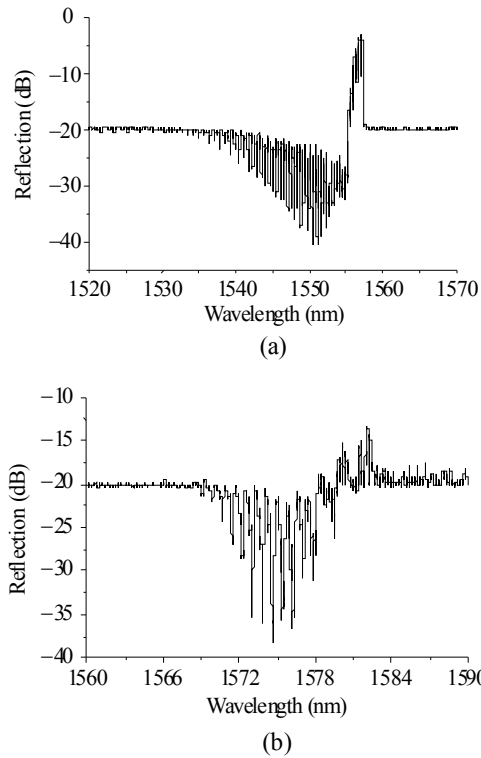
(a)

(b)

Fig. 7 Reflective spectra of (a) SMF R-TFBG and (b) GI-MMF R-TFBG sensors.

Further, the temperature responses of these two sensors were tested. By an automatically-controlled temperature test chamber, the temperature was raised from 26 ℃ to 106 ℃. The reflective spectra were recorded every 20 ℃, as shown in Figs. 8(a) and 8(b). The resonant notches with the largest contrast were chosen, and their shifts as a function of the temperature were measured, as shown in Figs. 9(a) and 9(b), respectively. The selected resonant notch could be identified by the peak counting method, as all the resonant notches had the same temperature sensitivity, and the total number of the notches would not change during the sensing process. The temperature sensitivities of the R-TFBG in the SMF and GI-MMF were 10 pm/℃ and 11 pm/℃, respectively. Both of them had the good linearity of 0.9999 and 0.9998, respectively. It was also indicated by the experimental results that the temperature sensitivity of the Bragg wavelength in the R-TFBG in the SMF was the same as that of the resonant notches.
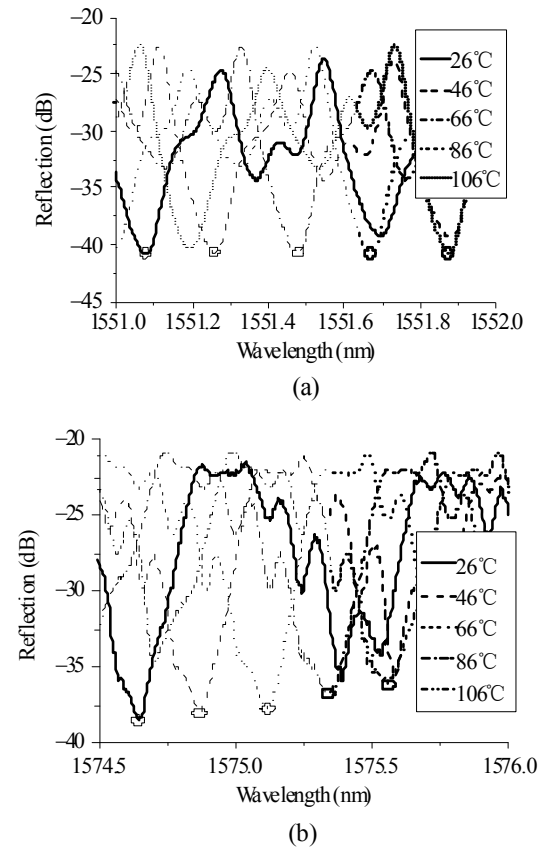

(a)

(b)

Fig. 8 Expanded reflective spectra of (a) SMF R-TFBG and (b) GI-MMF R-TFBG sensors at different temperatures.
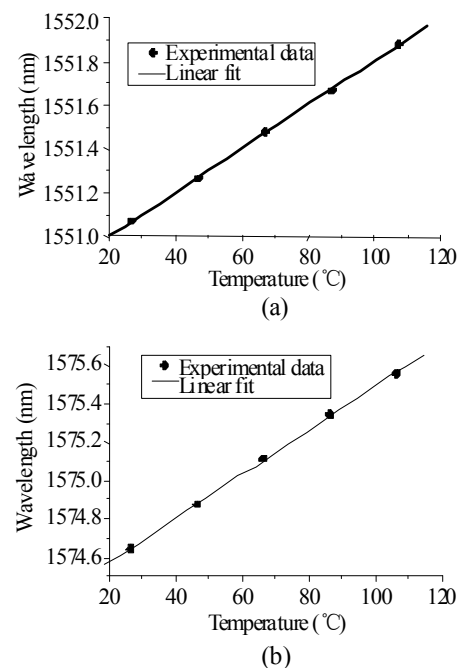

(a)

(b)

Fig. 9 Wavelength shift of the resonant notch with the maximum contrast as a function of the temperature: (a) SMF R-TFBG and (b) GI-MMF R-TFBG.

3. Conclusions

In conclusion, the tilted fiber Bragg gratings have been inscribed in the graded-index multimode fibers, and the sensing performance has been analyzed. Using the Fresnel reflection, the reflective tilted fiber Bragg gratings have been fabricated in both the hydrogen-loaded single mode fiber and graded-index multimode fiber. The reflective spectra have been analyzed, and the temperature sensing performance has also been investigated. These sensors had a small size and were easy to be fabricated and used.

Acknowledgment

References

[1] K. Zhou, L. Zhang, X. Chen, and I. Bennion, "Optic sensors of high refractive index responsivity and low thermal cross sensitivity utilizing fiber Bragg gratings of >80° -tilted structures," *Optics Letters*, vol. 31, no. 9, pp. 1193–1195, 2006.

[2] Y. Miao, B. Liu, K. Zhang, Y. Liu, H. Sun, and Q. Zhao, "Weakly tilted fibre Bragg grating inscription in all-solid photonic bandgap fibres," *Electronics Letters*, vol. 47, no. 4, pp. 275–277, 2011.

[3] Y. X. Jin, C. C. Chan, X. Y. Dong, and Y. F. Zhang, "Temperature-independent bending sensor with tilted fiber Bragg grating interacting with multimode fiber," *Optics Communications*, vol. 282, no. 19, pp. 3905–3907, 2009.

[4] L. Y. Shao, A. Laronche, M. Smietana, P. Mikulic, W. J. Bock, and J. Albert, "Highly sensitive bend sensor with hybrid long-period and tilted fiber Bragg grating," *Optics Communications*, vol. 283, no. 13, pp. 2690–2694, 2010.

[5] T. Guo, A. Ivanov, G. Chen, and J. Albert, "Temperature-independent tilted fiber grating vibration sensor based on cladding-core recoupling," *Optics Letters*, vol. 33, no. 9, pp. 1004–1006, 2008.

[6] T. Guo, H. Y. Tam, P. A. Krug, and J. Albert, "Reflective tilted fiber Bragg grating refractometer based on strong cladding to core recoupling," *Optics Express*, vol. 17, no. 7, pp. 5736–5742, 2009.

[7] B. Zhou, A. P. Zhang, S. H. He, and B. B. Gu, "Cladding-mode-recoupling-based tilted fiber Bragg grating sensor with a core-diameter-mismatched fiber section," *IEEE Photonics Journal*, vol. 2, pp. 152–157, 2010.

[8] T. Guo, L. Shao, H. Y. Tam, P. A. Krug, and J. Albert, "Tilted fiber grating accelerometer incorporating an abrupt biconical taper for cladding to core recoupling," *Optics Express*, vol. 17, no. 23, pp. 20651–20660, 2009.

[9] X. Y. Dong, H. Zhang, B. Liu, and Y. P. Miao, "Tilted fiber Bragg gratings: principle and sensing applications," *Photonic Sensors*, vol. 1, no. 1, pp. 6–30, 2011.

[10] A. P. Zhang, S. R. Gao, G. F. Yan, and Y. B. Bai, "Advance in optical fiber Bragg grating sensor technologies," *Photonic Sensors*, vol. 2, no. 1, pp. 1–13, 2012.

[11] Z. M. Liu, J. Liu, J. J. Zheng, L. Y. Fan, W. W. Jiang, and S. S. Jian, "Fabrication of optical fiber Bragg grating assisted mismatched coupler," *Chinese Physics Letters*, vol. 27, no. 1, pp. 014210, 2010.

[12] Y. Zhou, X. F. He, J. Yuan, L. Q. Yin, X. Y. Fang, and M. S. Cao, "Influence of non-uniform temperature field on spectra of fibre Bragg grating," *Chinese Physics Letters*, vol. 26, no. 1, pp. 014215, 2009.

[13] K. H. Wanser, K. F. Voss, and A. D. Kersey, "Novel fiber devices and sensors based on multimode fiber Bragg gratings," in *Proc. SPIE*, vol. 2360, pp. 265, 1994.

[14] T. Mizunami, V. Tzvetanka, T. Niiho, and S. Gupta, "Bragg gratings in multimode and few-mode optical fibers," *Journal of Lightwave Technology*, vol. 18, no. 2, pp. 230–235, 2000.

[15] T. Szkopek, V. Pasupathy, J. E. Sipe, and P. W. E. Smith, "Novel multimode fibre for narrowband

Bragg grating response," *IEEE Journal of Selected Topics in Quantum Electronics*, vol. 7, no. 3, pp. 425–429, 2001.

[16] K. Zhou, A. G. Simpson, L. Zhang, and I. Bennion, "Side-detection of strong radiation mode out-coupling from blazed FBGs in single-mode and multi-mode fibers," *IEEE Photonics Technology Letters*, vol. 15, no. 7, pp. 936–938, 2003.

[17] X. F. Yang C. L. Zhao, J. Q. Zhou, and G. Xin, "The characteristics of fiber slanted gratings in multimode fiber," *Optics Communications*, vol. 229, no. 1–6, pp. 161–165, 2004.

[18] X. F. Chen, K. M. Zhou, L. Zhang, and I. Bennoin, "Optical chemsensor based on etched tiled Bragg grating structures in multimode fiber," *IEEE Photonics Technology Letters*, vol. 17, no. 4, pp. 864–866, 2005.

[19] Y. Gong, T. Zhao, Y. J. Rao, and Y. Wu, "All-fiber curvature sensor based on multimode interference," *IEEE Photonics Technology Letters*, vol. 23, no. 11, pp. 679–681, 2011.